Lawrence Berkeley National Laboratory
Lawrence Berkeley National Laboratory

Title

Multi-strange baryon production in Au-Au collisions at sqrt(sNN) = 130 GeV

Permalink

https://escholarship.org/uc/item/0s97t1fm

Authors

Adams, J.
Adler, C.
Aggarwal, M.M.
et al.

Publication Date

2003-07-31

Multi-Strange Baryon Production in Au-Au collisions at $\sqrt{s_{NN}} = 130$ GeV

J. Adams,[3] C. Adler,[12] M.M. Aggarwal,[25] Z. Ahammed,[28] J. Amonett,[17] B.D. Anderson,[17] M. Anderson,[5] D. Arkhipkin,[11] G.S. Averichev,[10] S.K. Badyal,[16] J. Balewski,[13] O. Barannikova,[28, 10] L.S. Barnby,[17] J. Baudot,[15] S. Bekele,[24] V.V. Belaga,[10] R. Bellwied,[41] J. Berger,[12] B.I. Bezverkhny,[43] S. Bhardwaj,[29] P. Bhaskar,[38] A.K. Bhati,[25] H. Bichsel,[40] A. Billmeier,[41] L.C. Bland,[2] C.O. Blyth,[3] B.E. Bonner,[30] M. Botje,[23] A. Boucham,[34] A. Brandin,[21] A. Bravar,[2] R.V. Cadman,[1] X.Z. Cai,[33] H. Caines,[43] M. Calderón de la Barca Sánchez,[2] J. Carroll,[18] J. Castillo,[18] M. Castro,[41] D. Cebra,[5] P. Chaloupka,[9] S. Chattopadhyay,[38] H.F. Chen,[32] Y. Chen,[6] S.P. Chernenko,[10] M. Cherney,[8] A. Chikanian,[43] B. Choi,[36] W. Christie,[2] J.P. Coffin,[15] T.M. Cormier,[41] J.G. Cramer,[40] H.J. Crawford,[4] D. Das,[38] S. Das,[38] A.A. Derevschikov,[27] L. Didenko,[2] T. Dietel,[12] X. Dong,[32, 18] J.E. Draper,[5] F. Du,[43] A.K. Dubey,[14] V.B. Dunin,[10] J.C. Dunlop,[2] M.R. Dutta Majumdar,[38] V. Eckardt,[19] L.G. Efimov,[10] V. Emelianov,[21] J. Engelage,[4] G. Eppley,[30] B. Erazmus,[34] M. Estienne,[34] P. Fachini,[2] V. Faine,[2] J. Faivre,[15] R. Fatemi,[13] K. Filimonov,[18] P. Filip,[9] E. Finch,[43] Y. Fisyak,[2] D. Flierl,[12] K.J. Foley,[2] J. Fu,[42] C.A. Gagliardi,[35] M.S. Ganti,[38] T.D. Gutierrez,[5] N. Gagunashvili,[10] J. Gans,[43] L. Gaudichet,[34] M. Germain,[15] F. Geurts,[30] V. Ghazikhanian,[6] P. Ghosh,[38] J.E. Gonzalez,[6] O. Grachov,[41] V. Grigoriev,[21] S. Gronstal,[8] D. Grosnick,[37] M. Guedon,[15] S.M. Guertin,[6] A. Gupta,[16] E. Gushin,[21] T.J. Hallman,[2] D. Hardtke,[18] J.W. Harris,[43] M. Heinz,[43] T.W. Henry,[35] S. Heppelmann,[26] T. Herston,[28] B. Hippolyte,[43] A. Hirsch,[28] E. Hjort,[18] G.W. Hoffmann,[36] M. Horsley,[43] H.Z. Huang,[6] S.L. Huang,[32] T.J. Humanic,[24] G. Igo,[6] A. Ishihara,[36] P. Jacobs,[18] W.W. Jacobs,[13] M. Janik,[39] I. Johnson,[18] P.G. Jones,[3] E.G. Judd,[4] S. Kabana,[43] M. Kaneta,[18] M. Kaplan,[7] D. Keane,[17] J. Kiryluk,[6] A. Kisiel,[39] J. Klay,[18] S.R. Klein,[18] A. Klyachko,[13] D.D. Koetke,[37] T. Kollegger,[12] A.S. Konstantinov,[27] M. Kopytine,[17] L. Kotchenda,[21] A.D. Kovalenko,[10] M. Kramer,[22] P. Kravtsov,[21] K. Krueger,[1] C. Kuhn,[15] A.I. Kulikov,[10] A. Kumar,[25] G.J. Kunde,[43] C.L. Kunz,[7] R.Kh. Kutuev,[11] A.A. Kuznetsov,[10] M.A.C. Lamont,[3] J.M. Landgraf,[2] S. Lange,[12] C.P. Lansdell,[36] B. Lasiuk,[43] F. Laue,[2] J. Lauret,[2] A. Lebedev,[2] R. Lednický,[10] V.M. Leontiev,[27] M.J. LeVine,[2] C. Li,[32] Q. Li,[41] S.J. Lindenbaum,[22] M.A. Lisa,[24] F. Liu,[42] L. Liu,[42] Z. Liu,[42] Q.J. Liu,[40] T. Ljubicic,[2] W.J. Llope,[30] H. Long,[6] R.S. Longacre,[2] M. Lopez-Noriega,[24] W.A. Love,[2] T. Ludlam,[2] D. Lynn,[2] J. Ma,[6] Y.G. Ma,[33] D. Magestro,[24] S. Mahajan,[16] L.K. Mangotra,[16] D.P. Mahapatra,[14] R. Majka,[43] R. Manweiler,[37] S. Margetis,[17] C. Markert,[43] L. Martin,[34] J. Marx,[18] H.S. Matis,[18] Yu.A. Matulenko,[27] T.S. McShane,[8] F. Meissner,[18] Yu. Melnick,[27] A. Meschanin,[27] M. Messer,[2] M.L. Miller,[43] Z. Milosevich,[7] N.G. Minaev,[27] C. Mironov,[17] D. Mishra,[14] J. Mitchell,[30] B. Mohanty,[38] L. Molnar,[28] C.F. Moore,[36] M.J. Mora-Corral,[19] V. Morozov,[18] M.M. de Moura,[41] M.G. Munhoz,[31] B.K. Nandi,[38] S.K. Nayak,[16] T.K. Nayak,[38] J.M. Nelson,[3] P. Nevski,[2] V.A. Nikitin,[11] L.V. Nogach,[27] B. Norman,[17] S.B. Nurushev,[27] G. Odyniec,[18] A. Ogawa,[2] V. Okorokov,[21] M. Oldenburg,[18] D. Olson,[18] G. Paic,[24] S.U. Pandey,[41] S.K. Pal,[38] Y. Panebratsev,[10] S.Y. Panitkin,[2] A.I. Pavlinov,[41] T. Pawlak,[39] V. Perevoztchikov,[2] W. Peryt,[39] V.A. Petrov,[11] S.C. Phatak,[14] R. Picha,[5] M. Planinic,[44] J. Pluta,[39] N. Porile,[28] J. Porter,[2] A.M. Poskanzer,[18] M. Potekhin,[2] E. Potrebenikova,[10] B.V.K.S. Potukuchi,[16] D. Prindle,[40] C. Pruneau,[41] J. Putschke,[19] G. Rai,[18] G. Rakness,[13] R. Raniwala,[29] S. Raniwala,[29] O. Ravel,[34] R.L. Ray,[36] S.V. Razin,[10, 13] D. Reichhold,[28] J.G. Reid,[40] G. Renault,[34] F. Retiere,[18] A. Ridiger,[21] H.G. Ritter,[18] J.B. Roberts,[30] O.V. Rogachevski,[10] J.L. Romero,[5] A. Rose,[41] C. Roy,[34] L.J. Ruan,[32, 2] R. Sahoo,[14] I. Sakrejda,[18] S. Salur,[43] J. Sandweiss,[43] I. Savin,[11] J. Schambach,[36] R.P. Scharenberg,[28] N. Schmitz,[19] L.S. Schroeder,[18] K. Schweda,[18] J. Seger,[8] D. Seliverstov,[21] P. Seyboth,[19] E. Shahaliev,[10] M. Shao,[32] M. Sharma,[25] K.E. Shestermanov,[27] S.S. Shimanskii,[10] R.N. Singaraju,[38] F. Simon,[19] G. Skoro,[10] N. Smirnov,[43] R. Snellings,[23] G. Sood,[25] P. Sorensen,[6] J. Sowinski,[13] H.M. Spinka,[1] B. Srivastava,[28] S. Stanislaus,[37] R. Stock,[12] A. Stolpovsky,[41] M. Strikhanov,[21] B. Stringfellow,[28] C. Struck,[12] A.A.P. Suaide,[41] E. Sugarbaker,[24] C. Suire,[2] M. Šumbera,[9] B. Surrow,[2] T.J.M. Symons,[18] A. Szanto de Toledo,[31] P. Szarwas,[39] A. Tai,[6] J. Takahashi,[31] A.H. Tang,[2, 23] D. Thein,[6] J.H. Thomas,[18] V. Tikhomirov,[21] M. Tokarev,[10] M.B. Tonjes,[20] T.A. Trainor,[40] S. Trentalange,[6] R.E. Tribble,[35] M.D. Trivedi,[38] V. Trofimov,[21] O. Tsai,[6] T. Ullrich,[2] D.G. Underwood,[1] G. Van Buren,[2] A.M. VanderMolen,[20] A.N. Vasiliev,[27] M. Vasiliev,[35] S.E. Vigdor,[13] Y.P. Viyogi,[38] S.A. Voloshin,[41] W. Waggoner,[8] F. Wang,[28] G. Wang,[17] X.L. Wang,[32] Z.M. Wang,[32] H. Ward,[36] J.W. Watson,[17] R. Wells,[24] G.D. Westfall,[20] C. Whitten Jr.,[6] H. Wieman,[18] R. Willson,[24] S.W. Wissink,[13] R. Witt,[43] J. Wood,[6] J. Wu,[32] N. Xu,[18] Z. Xu,[2] Z.Z. Xu,[32] A.E. Yakutin,[27] E. Yamamoto,[18] J. Yang,[6] P. Yepes,[30] V.I. Yurevich,[10] Y.V. Zanevski,[10] I. Zborovský,[9] H. Zhang,[43, 2] H.Y. Zhang,[17] W.M. Zhang,[17] Z.P. Zhang,[32] P.A. Żołnierczuk,[13] R. Zoulkarneev,[11] J. Zoulkarneeva,[11] and A.N. Zubarev[10]

(STAR Collaboration)[,*]

[1]*Argonne National Laboratory, Argonne, Illinois 60439*
[2]*Brookhaven National Laboratory, Upton, New York 11973*
[3]*University of Birmingham, Birmingham, United Kingdom*
[4]*University of California, Berkeley, California 94720*
[5]*University of California, Davis, California 95616*
[6]*University of California, Los Angeles, California 90095*
[7]*Carnegie Mellon University, Pittsburgh, Pennsylvania 15213*
[8]*Creighton University, Omaha, Nebraska 68178*
[9]*Nuclear Physics Institute AS CR, Řež/Prague, Czech Republic*
[10]*Laboratory for High Energy (JINR), Dubna, Russia*
[11]*Particle Physics Laboratory (JINR), Dubna, Russia*
[12]*University of Frankfurt, Frankfurt, Germany*
[13]*Indiana University, Bloomington, Indiana 47408*
[14]*Insitute of Physics, Bhubaneswar 751005, India*
[15]*Institut de Recherches Subatomiques, Strasbourg, France*
[16]*University of Jammu, Jammu 180001, India*
[17]*Kent State University, Kent, Ohio 44242*
[18]*Lawrence Berkeley National Laboratory, Berkeley, California 94720*
[19]*Max-Planck-Institut für Physik, Munich, Germany*
[20]*Michigan State University, East Lansing, Michigan 48824*
[21]*Moscow Engineering Physics Institute, Moscow Russia*
[22]*City College of New York, New York City, New York 10031*
[23]*NIKHEF, Amsterdam, The Netherlands*
[24]*Ohio State University, Columbus, Ohio 43210*
[25]*Panjab University, Chandigarh 160014, India*
[26]*Pennsylvania State University, University Park, Pennsylvania 16802*
[27]*Institute of High Energy Physics, Protvino, Russia*
[28]*Purdue University, West Lafayette, Indiana 47907*
[29]*University of Rajasthan, Jaipur 302004, India*
[30]*Rice University, Houston, Texas 77251*
[31]*Universidade de Sao Paulo, Sao Paulo, Brazil*
[32]*University of Science & Technology of China, Anhui 230027, China*
[33]*Shanghai Institute of Nuclear Research, Shanghai 201800, P.R. China*
[34]*SUBATECH, Nantes, France*
[35]*Texas A&M, College Station, Texas 77843*
[36]*University of Texas, Austin, Texas 78712*
[37]*Valparaiso University, Valparaiso, Indiana 46383*
[38]*Variable Energy Cyclotron Centre, Kolkata 700064, India*
[39]*Warsaw University of Technology, Warsaw, Poland*
[40]*University of Washington, Seattle, Washington 98195*
[41]*Wayne State University, Detroit, Michigan 48201*
[42]*Institute of Particle Physics, CCNU (HZNU), Wuhan, 430079 China*
[43]*Yale University, New Haven, Connecticut 06520*
[44]*University of Zagreb, Zagreb, HR-10002, Croatia*
(Dated: July 30, 2003)

The transverse mass spectra and mid-rapidity yields for Ξs and Ωs plus their anti-particles are presented. The 10% most central collision yields suggest that the amount of multi-strange particles produced per produced charged hadron increases from SPS to RHIC energies. A hydrodynamically inspired model fit to the spectra, which assumes a thermalized source, seems to indicate that these multi-strange particles experience a significant transverse flow effect, but are emitted when the system is hotter and the flow is smaller than values obtained from a combined fit to π, K, p and Λs.

PACS numbers:

In heavy ion collisions we aim to investigate nuclear matter under extreme conditions of pressure and temperature which is expected to lead to the creation of deconfined partonic matter, the Quark Gluon Plasma (QGP) [1]. The study of strange particles production is thought to yield information on the collision dynamics from the early stage to chemical and thermal freeze-out. The production of strangeness through partonic interactions, mainly $gg \to s\bar{s}$, is expected to dominate over that by hadronic scatterings [2, 3]. Since at RHIC energies the initial gluon density is expected to be much higher than in lower-energy heavy ion collisions [4, 5], strange

particles, especially multi-strange particles are expected to be more sensitive to the partonic dynamics of the early stage of the collision.

Chemical freeze-out is defined by the temperature, T_{ch}, at which inelastic collisions cease and the relative particle ratios become fixed. With no strange quarks in the initial state it is possible for the system to freeze-out chemically before absolute strangeness chemical equilibrium has been reached. Statistical models have had much success in reproducing the particle ratios both at lower energies (e.g. [6, 7, 8]) and at RHIC (e.g. [9, 10]). Some of these models, which assume chemical equilibrium, allow for the possibility of non-equilibrium in the strangeness channel by the introduction of a strangeness saturation factor, γ_s [7, 10]. This factor reaches unity when complete strangeness saturation, or absolute chemical equilibrium, is present in the system. A common T_{ch} of 170 MeV [9] is indicated by fits to measurements at 130 GeV of anti-baryon to baryon ratios as well as particle ratios involving only mesons and non-strange baryons. This temperature is remarkably close to that of the phase transition calculated with lattice QCD [11]. Re-calculating the fits with the inclusion of the multi-strange baryons allows a more sensitive test of statistical models to be made.

A comprehensive analysis of the transverse momentum or transverse mass spectra allows us to probe the possibility of thermal equilibrium of the system. The high mass of the multi-strange baryons means they are more sensitive to the size of the transverse flow of the system. It has previously been suggested that thermal freeze-out occurs much earlier for Ω and Ξ than for lower mass particles due to the predicted low scattering cross section of Ω and Ξ [12]. In the limit of vanishing cross sections this would mean that these particles are emitted almost directly from the phase boundary of the hadronizing fireball. However, these cross sections have not actually been measured and may not be negligible. If they were significant, combined with the now sizeable particle production at these energies, the $\Omega + X$ elastic collision rate would delay the Ω kinetic freeze-out, resulting in these particles carrying the same flow velocity as the pions and kaons. By comparing different thermal freeze-out scenarios to the data (e.g. [13, 14, 15]) it may be possible to determine the rate of build-up of radial flow.

The data presented here were taken with the STAR detector in Au+Au collisions at $\sqrt{s_{NN}} = 130$ GeV. The main tracking detector is a large cylindrical Time Projection Chamber. A Central Trigger Barrel measuring the produced charged particle multiplicity around mid-rapidity plus two Zero Degree Calorimeters essentially measuring neutral spectator energy were used for triggering [16]. In this paper the centrality of the collisions is determined from the measured mid-rapidity negative particle multiplicity. The data were divided into three centrality classes corresponding to 0-10%, 10-25% and
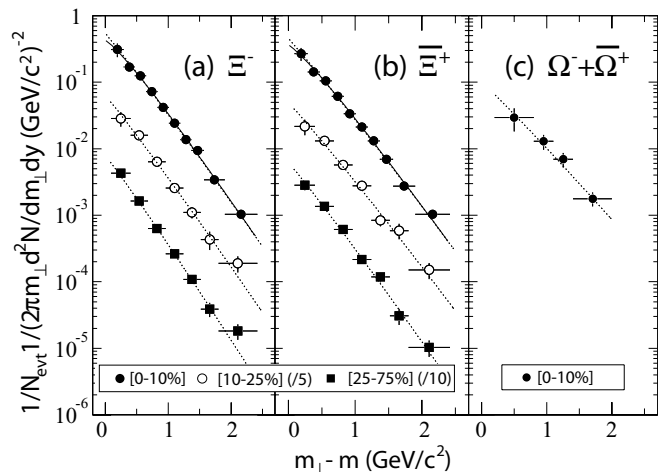

FIG. 1: $m_\perp$ spectra for (a) Ξ^-, (b) $\overline{\Xi}^+$ and (c) Ω as a function of centrality. Scale factors have been applied to the spectra for clarity. Points are drawn at the bin center. The horizontal bars indicate the bin size. The dashed curves are Boltzmann fits to the spectra. The solid curves are hydrodynamically inspired model fits to the most central Ξ^- and $\overline{\Xi}^+$ spectra.

h^-		Exponential		Boltzmann	
		dN/dy	T_E(MeV)	dN/dy	T_B(MeV)
	Ξ^-	2.16±0.09	338±6	2.06±0.09	296±5
260.3±7.5	$\overline{\Xi}^+$	1.81±0.08	339±7	1.73±0.08	297±5
	Ω	0.59±0.14	417±52	0.58±0.14	362±39
163.6±5.2	Ξ^-	1.22±0.11	335±16	1.18±0.11	291±13
	$\overline{\Xi}^+$	1.00±0.10	349±17	0.97±0.10	302±13
42.5±3.0	Ξ^-	0.28±0.02	312±12	0.27±0.02	273±10
	$\overline{\Xi}^+$	0.23±0.02	320±11	0.22±0.02	280±9

TABLE I: Fit parameters for the $m_\perp$ spectra of the Ξ^-, $\overline{\Xi}^+$ and Ω. The data represent the 0-10%, 10-25% and 25-75% centrality bins with $h^- = dN_{h^-}/d\eta|_{|\eta|<0.5}$. Only statistical and $p_\perp$ dependent systematic uncertainties are presented. The $p_\perp$ independent systematic uncertanties are 10%.

25-75% of the total hadronic cross section as described in [17]. Multi-strange particles are identified via their decay modes $\Xi \rightarrow \Lambda + \pi$ and $\Omega \rightarrow \Lambda + K$ with the subsequent decay of $\Lambda \rightarrow p + \pi$. The tertiary Λ vertex is identified by selecting positive and negative tracks that are consistent with an origin at the decay of a hyperon some distance from the primary collision point [18]. The secondary vertex of the decay is located in a similar fashion by combining the previously identified Λ with a charged particle. Simple cuts on geometry, kinematics and particle identification, via specific ionization, are applied at each step to reduce the background due to the high multiplicity [17]. The momenta of the daughter particles at the decay vertex are then combined to cal-
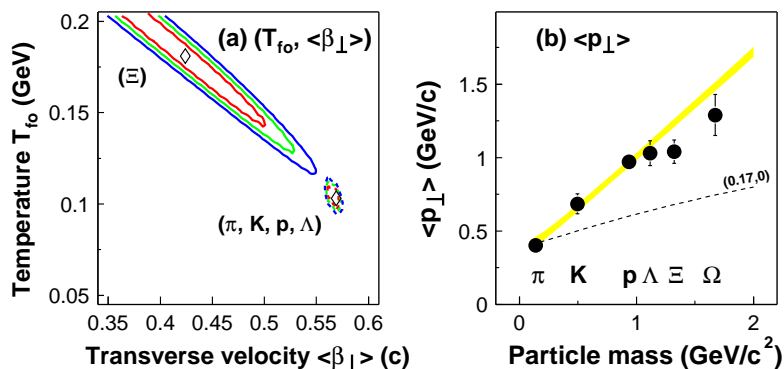
FIG. 2: (a) The kinetic freeze-out temperature vs transverse flow velocity for the hydrodynamically inspired model fits to the $m_\perp$ spectra. The 1, 2 and 3 sigma contours are shown. Solid curves are for a simultaneous fit to the Ξ^- and $\overline{\Xi}^+$. Dashed curves are a separate fit to the STAR π, K, p and Λ data. The diamonds represent the best fit in both cases. (b) Mean transverse momenta for identified particles vs particle mass (see text for details). The band results from the three sigma contour of the hydrodynamically inspired model fit to the π, K, p and Λ data and the dashed curve is for $T_{\mathrm{fo}} = 170$ MeV, $< \beta_\perp >= 0$.

culate the parent particle kinematics. The peaks in the invariant mass plots have an average signal to noise ratio of 0.74, 0.78 and 0.86 for the Ξ^-, $\overline{\Xi}^+$ and Ω respectively in the 0-10% centrality bin. The signal to noise ratios are calculated for ± 15 MeV/c^2 about the expected mass. The statistics of the Ω^- and $\overline{\Omega}^+$ signal are not sufficient to allow a separate measurement of the spectra of each particle. Hence Ω refers to Ω^- plus $\overline{\Omega}^+$. The momentum integrated $\overline{\Omega}^+/\Omega^-$ ratio for the top 11% most central data is $0.95 \pm 0.15(stat) \pm 0.05(sys)$ [19].

The invariant mass distributions are histogramed in transverse mass, $m_\perp = \sqrt{p_\perp^2 + m^2}$, and the signal extracted for each bin. The raw yields are calculated from the invariant mass distributions by counting the entries within ± 15 MeV/c^2 about the expected mass and then subtracting the background. The background is estimated by sampling two regions on either side of the peak. The raw yield in each $m_\perp$ bin is corrected for detector acceptance and reconstruction efficiency by the Monte Carlo technique, where simulated particles were embedded into real events. The data cover $\mid y \mid < 0.75$, where efficiency and acceptance studies have shown the corrections to be constant. The total correction factors for the $\Xi(\Omega)$ are 0.2%(0.04%) for the lowest $m_\perp$ bin rising to 4.0%(0.5%) for the highest bin.

Fig. 1 shows the invariant $m_\perp$ spectra as functions of centrality for the Ξ^- and $\overline{\Xi}^+$, and the Ω for the 10% most central data. A portion of the systematic uncertainties are a function of $p_\perp$, therefore this uncertainty is added in quadrature, on a bin-by-bin basis, to the statistical one, yielding the vertical bars in Fig. 1. We estimate the remaining systematic uncertainties to be 10% on both the extracted invariant yields and slope parameters, the major source of which lies in the misrepresentation of the embedded Monte-Carlo to the data resulting in a system-

atic uncertainty in the efficiency calculation. These were obtained by exploring the dependence of the invariant yields and slope parameters to changes in the cuts phase space (more details can be found in [20, 21, 22]). The weak decay feed-down of Ω on Ξ is estimated to be less than 2% and thus is neglected.

Table I shows the results of fitting the $m_\perp$ spectra by an exponential ($A_E e^{-(m_\perp - m)/T_E}$) and Boltzmann ($A_B m_\perp e^{-(m_\perp - m)/T_B}$) functions. Both functions give a good representation of the data but the Boltzmann fit gives a slightly better χ^2/dof. The inverse slopes of the Ξ particles are the same within uncertainties and show no apparent increase over the measured centralities. The yields per unit of rapidity are extracted by integrating each function over the entire $m_\perp$ range. The measured Ξ spectra correspond to $\sim 75\%$ of the total yield and the Ω to $\sim 66\%$. The Ξ^- and $\overline{\Xi}^+$ yields as function of $h^- = dN_{h^-}/d\eta|_{|\eta|<0.5}$ appear linear; such behavior was reported for the Λ hyperon at RHIC [18].

The 10% most central $m_\perp$ spectra are also fit by a hydrodynamically inspired function [23]. In this model, all considered particles are emitted from a thermal expanding source with a transverse flow velocity $< \beta_\perp >$ at the thermal freeze-out temperature T_{fo}. As in [24] a flow velocity profile of $\beta_\perp(r) = \beta_s(r/R)^{0.5}$ is used, where R is the maximum emission radius. The solid lines of Fig. 2(a) show the one, two and three sigma contours for T_{fo} vs $< \beta_\perp >$ for the fit to the Ξ^- and $\overline{\Xi}^+$ data combined, with the diamond indicating the best fit solution ($T_{\mathrm{fo}} = 182 \pm 29$ MeV, $< \beta_\perp >= 0.42 \pm 0.06$ c, $\chi^2/dof = 13/15$). Also shown, as the dashed lines, are the one, two and three sigma contours for a combined fit to the STAR π, K, p, and Λ data [18, 24, 25, 26], and the marker is the optimal fit location. Clearly the results for the two data sets do not overlap indicating that the Ξ

baryons, within this approach, show a different thermal freeze-out behavior than π, K, p, and Λ. The current Ω statistics do not allow to distinguish between an early decoupling or a common freeze-out with the lighter species. Fig. 2(b) shows the mean $p_\perp$ for these particles calculated from the functions which best reproduce each $m_\perp$ spectrum (Bose-Einstein for π, exponential for K, hydrodynamically inspired function for p and Boltzmann for Λ, Ξ and Ω). The error bars on the experimental points are statistical and systematic uncertainties added in quadrature. The band represents the model prediction based on the three sigma contour for the fit to the STAR π, K, p, and Λ data while the lower dashed curve shows the prediction for $T_{\rm fo}$=170 MeV, $<\beta_\perp>$=0, *i.e.* a system where thermal and chemical freeze-out coincide and no transverse flow is developed. From Fig. 2(a) it is likely that the Ξ baryons prefer a hotter thermal freeze-out temperature parameter when compared to that resulting from fits to the lower mass particles. This is consistent with the calculated $<p_\perp>$ of the Ξ and Ωs being below the solid band in Fig. 2(b).

If, as indicated by this fit, the Ξ thermal freeze-out occurs in conjunction with that of chemical freeze-out, $T_{\rm ch} \sim$170 MeV, this could be an indication that a significant fraction of the collective transverse flow has already developed at/before chemical freeze-out, probably at a partonic stage. Two alternative models have also been proposed for describing the RHIC spectra. The first [14] assumes that all transverse radial flow is developed at/before $T_{\rm ch}=T_{\rm fo}$=165 MeV. The apparent softening of the lighter mass spectra is then due to contamination from resonance decay products. A hydrodynamical approach [27] is used in the second scenario where the particle mean free paths are assumed small until thermal freeze-out around $T_{\rm fo}$=110 MeV. These large cross-sections result in even the Ω developing a sizeable fraction of its radial flow after hadronization.

The $\overline{\Xi}^+/h^-$ and $\overline{\Lambda}/h^-$ ratios for the most central data, as shown in Fig. 3(a), increase from SPS energies [28] to RHIC, whereas the Ξ^-/h^- ratio stays constant and the Λ/h^- decreases. When discussing the baryon ratios the interplay of increased strangeness production and reduction in the net-baryon number, which was significant at the SPS, has to be considered. The proximity of the net-baryon number to zero at RHIC is reflected in the fact that the ratio of Ξ^-/h^- is close to $\overline{\Xi}^+/h^-$. The reduction in the net-baryon number has a larger effect on the Λ than on the Ξ^-, as seen in Fig 3(a), and thus creates the observed rise in the Ξ^-/Λ ratio (Fig. 3(b)). It is interesting to note that the $\overline{\Xi}^+/\overline{\Lambda}$ ratio is a constant from SPS to RHIC indicating that the scale of the multi-strange enhancement is the same for singly and doubly strange baryons.

A fit to the reported 0-10% centrality particle ratios from STAR [18, 19, 24, 25, 26, 29], including the multi-
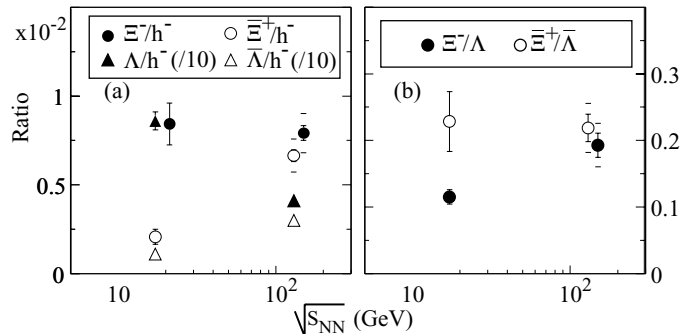

FIG. 3: (a) Ξ^-, $\overline{\Xi}^+$, Λ and $\overline{\Lambda}$ to h^- ratios and (b) Ξ^-/Λ and $\overline{\Xi}^+/\overline{\Lambda}$ ratios for the most central data as a function of $\sqrt{s_{NN}}$. The solid lines indicate the statistical uncertainty while the caps indicate the statistical and systematic uncertainties added in quadrature. Some ratios are slightly shifted along the x-axis for clarity.

Ratio ($\times 10^{-3}$)	Data 0-10%	Stat.	Non-Equil.	HIJING/$B\overline{B}$
Ξ^-/h^-	7.9±0.4±1.0	7.7	7.6	5.1
$\overline{\Xi}^+/h^-$	6.6±0.3±0.8	6.5	6.1	3.0
Ω/h^-	2.2±0.5±0.4	2.9	2.8	0.29
Ξ^-/Λ	193±18±27	148	190	171
$\overline{\Xi}^+/\overline{\Lambda}$	219±21±31	163	207	142

TABLE II: Ratios from the 10% most central data compared to predictions from a statistical model[10] a non-equilibrium model[30] and HIJING/$B\overline{B}$[31]. Uncertainties shown are first statistical and then systematic.

strange particle measurements, using the thermal model described in [10] results in a χ^2/dof of 8.5/9, a $T_{\rm ch}$ of 181±8 MeV, light quark and strange quark chemical potentials of 11.7±0.6 MeV and 0.9±1.6 MeV respectively, and γ_s=0.96±0.06. The fact that γ_s is equal to unity, within errors, when used as a free parameter in the model indicates that a saturation of strangeness production has been achieved in the most central collisions. Table II shows particle ratios for the 0-10% centrality bin compared to values from three different models: a fit corresponding to the statistical model used above, another corresponding to a statistical model that allows for chemical non-equilibrium via an over-saturation of both the light quark and strangeness phase spaces [30] and the prediction of the event generator HIJING/$B\overline{B}$ v1.0 which uses a gluon-junction mechanism to enhance the transport of baryons to mid-rapidity [31]. All ratios are well reproduced by both statistical models, indicating that the strangeness production is duplicated well by such approaches. HIJING/$B\overline{B}$, however, fails to predict the multi-strange to h^- ratios, in particular that of the Ω, which it under-predicts by nearly an order of magni-

tude. It has previously been shown that HIJING successfully predicts the mid-rapidity total charged particle yields [32] suggesting that the entropy is reasonably well reproduced by this model. The addition of the gluon-junction mechanism, which was necessary to replicate the small net baryon yields at RHIC [33], does not sufficiently enhance the multi-strange baryon yields suggesting that a different physics mechanism is necessary to model the strangeness production. At SPS energies the introduction of final state interactions helped to account for the observed hyperon enhancement but failed to reproduce the overall strangeness production (K^+/π^+). The introduction of strong partonic interactions in the initial state was needed to account for both the hyperon and overall strangeness production at the SPS [34].

In summary, the total yield of multi-strange baryons per h^- in Au-Au collisions is increased compared to that at the top SPS energies. A chemical analysis of the data indicates that for central collisions the strangeness phase space is now saturated. A fit of the $m_\perp$ spectra to a hydrodynamically inspired model suggests the Ξ baryons thermally freeze out of the rapidly expanding collision region at a hotter temperature, which is close to that of chemical freeze-out, and with a smaller transverse flow than the lighter particle species. This suggests that they decouple at an earlier stage of the collision and thus probe a different dynamical region, but one at which a sizeable fraction of the transverse flow has already developed. All these observations are compatible with the early stage of the collision being driven by partonic interactions.

[*] URL: www.star.bnl.gov

[1] For reviews and recent developments see *"Quark Matter '2002"*, Nucl. Phys. **A715**, 1c (2003).

[2] J. Rafelski and B. Müller, Phys. Rev. Lett. **48**, 1066 (1982).

[3] P. Koch, B. Müller and J. Rafelski, Phys. Rep. **142**, 167 (1986).

[4] J. Breitweg *et al.*, Eur. Phys. J. **C7**, 609 (1999).

[5] K. Kajantie, Nucl. Phys. **A663**, 191 (2000); K.J. Eskola and K. Kajantie, Z. Phys. **C75**, 515 (1997).

[6] P. Braun-Munzinger *et al.*, Phys. Lett. **B344**, 43 (1995).

[7] A. Keranen and F. Becattini, Phys. Rev. **C65**, 044901 (2002).

[8] P. Braun-Munzinger *et al.*, Phys. Lett. **B465**, 15 (1999).

[9] P. Braun-Munzinger *et al.*, Phys. Lett. **B518**, 41 (2001).

[10] N. Xu and M. Kaneta, Nucl. Phys. **A698**, 306 (2002).

[11] F. Karsch, Nucl. Phys. **A698**, 199 (2002).

[12] H. van Hecke, H. Sorge and N. Xu, Phys. Rev. Lett. **81**, 5764 (1998).

[13] K. Bugaev *et al.*, Phys. Lett. **B544**, 127 (2002) and Phys. Rev. Lett. **88**, 132301 (2002).

[14] W. Broniowski and W. Florkowski, Phys. Rev. Lett. **87**, 272302 (2001).

[15] D. Teaney, J. Lauret and E.V. Shuryak, nucl-th/0110037.

[16] STAR Collaboration, Nucl. Instrum. Meth. **A499**, 659 (2003).

[17] C. Adler *et al.*, Phys. Rev. Lett. **87**, 112303 (2001).

[18] C. Adler *et al.*, Phys. Rev. Lett. **89**, 092301 (2002).

[19] J. Adams *et al.*, Phys. Lett. **B567**, 167 (2003).

[20] C. Lansdell, Ph.D Thesis, University of Texas (2002).

[21] J. Castillo, Ph.D Thesis, Université de Paris 7 (2002).

[22] B. Hippolyte, Ph.D Thesis, Université de Strasbourg (2002).

[23] E. Schnedermann, J. Sollfrank and U. Heinz, Phys. Rev. **C48**, 2462 (1993).

[24] J. Adams *et al.*, to be submitted to Phys. Rev. Lett. [nucl-ex/0306029]

[25] C. Adler *et al.*, to be submitted to Phys. Lett. **B** [nucl-ex/0206008]

[26] J. Adams *et al.*, to be submitted to Phys. Rev. **C** (2003).

[27] P. F. Kolb and U. Heinz, nucl-th/0305084.

[28] E. Andersen *et al.*, J. Phys. G **25**, 171 (1999).

[29] C. Adler *et al.*, Phys. Rev. **C65**, 041901(R) (2002).

[30] J. Rafelski and J. Letessier, Nucl. Phys. **A715**, 98 (2003).

[31] X.N. Wang and M. Gyulassy, Phys. Rev. **D44**, 3501 (1991), S.E. Vance *et al.*, Phys. Lett. **B443**, 45 (1998).

[32] B.B. Back *et al.*, Phys. Rev. Lett. **87**, 102303 (2001).

[33] K. Adcox *et al.*, Phys. Rev. Lett. **89**, 092302 (2002).

[34] S. Vance, J. Phys. G **27**, 603 (2001).